Chemical Engineering Journal 452 (2023) 139280

Contents lists available at ScienceDirect

Chemical Engineering Journal

journal homepage: www.elsevier.com/locate/cej

Reversible acetalization of cellulose: A platform for bio-based materials with adjustable properties and biodegradation

Stefan Peil [a,b], Hubert Gojzewski [a], Frederik R. Wurm [a,*]

[a] Sustainable Polymer Chemistry (SPC), Department of Molecules and Materials, MESA+ Institute for Nanotechnology, Faculty of Science and Technology, University of Twente, 7500 AE Enschede, The Netherlands
[b] Max-Planck-Institut für Polymerforschung, Ackermannweg 10, 55128 Mainz, Germany

ARTICLE INFO

Keywords:
Acetalated
Biodegradable
Bio-based
Soil-degradable
Compost
Acetal-derivatized

ABSTRACT

Bio-based and biodegradable polymers are essential for a sustainable society. Cellulose is the most abundant biopolymer on earth; however, derivatization is necessary for its processing, which slows down its biodegradability dramatically, e.g. used cigarette filters made from cellulose acetate are barely biodegradable. We developed the first reversible modification of cellulose, which allows processing and guarantees full biodegradation even at high degrees of substitution as the linkers, acetals, can be cleaved first during the degradation process releasing native cellulose that biodegrades in a second step. Acetalization is a versatile platform approach to bio-based and fully degradable cellulose-derivatives, which are characterized by solubility in common organic solvents (alcohols, aromatic and chlorinated solvents), adjustable glass transition temperatures (-48 °C < T_g < 80 °C), young's modulus (1.9 MPa < E < 58 MPa) and contact angle (86° < θ < 124°). In contrast to previously known cellulose modifications, cellulose acetals remain fully degradable as the acetal bond is reversible and undergoes an acidic cleavage under desired conditions, for instance in compost, followed by enzymatic degradation of the remaining cellulose backbone. With climate change and plastic pollution, these new and versatile cellulose acetals provide bio-based and biodegradable alternatives to fossil-based and non-degradable polyolefin plastics, leading to a more sustainable future for our planet.

1. Introduction

Cellulose-based materials like "Cellophane" were one of the first man-made plastics, but now play a minor role in today's polymers, due to difficult processability and limited material properties. Common cellulose modifications, such as esterification, are capable of improving processability, however the modification of hydroxyl groups strongly reduces the biodegradation rates of modified cellulose. For example cellulose acetate (used in cigarette filters) has been reported to undergo only partial degradation over several years [1–3].

With the rise of synthetic polymers with widely adjustable properties and easy processability, they have become indispensable in multiple fields from medicine, packaging materials, cosmetics, coatings up to agriculture. Worldwide, over 350 million tons of synthetic plastics are produced annually and more than 8300 million tons of virgin polymers have been produced to date, of which almost 80 % have been discarded [4].

Worldwide accumulation of microplastics generated from littered, mostly petroleum-based polymers, in soil, rivers, the oceans and even in the polar regions makes clean up impossible and the need for biodegradable alternatives obvious [5]. The European Union recently restricted "the use of intentionally added microplastic particles to consumer or professional use products of any kind" [6].

Bio-based polymers such as cellulose are in the forefront of the next generation of modern plastics because of their inherent biodegradability. Natural occurring microorganisms in soil or waters evolved enzymes like cellulases, which are able to depolymerize the cellulose backbone and utilize the monomers as nutrition [7]. Cellulose, as the most abundant bio-based polymer on Earth, is cheap and belongs to the non-edible biomass making it an attractive renewable resource [8]. Annually, 400 million tons of cellulose are extracted in the paper industry alone [9].

However, strong hydrogen bonds and broad molar mass dispersity limits cellulose's processability and material properties. Chemical modification strategies for cellulose such as oxidation, esterification, etherification, urethanization, amidation and non-covalent

* Corresponding author.
E-mail address: Frederik.wurm@utwente.nl (F.R. Wurm).

https://doi.org/10.1016/j.cej.2022.139280
Received 23 July 2022; Received in revised form 8 September 2022; Accepted 14 September 2022
Available online 19 September 2022

modifications reduced the limitations in processability and expanded the material properties for cellulose-based materials. However, all chemical modifications to date decreased cellulose's biodegradability significantly [1,2,10].

Previous literature on other acetalated biopolymers, such as dextrans, reported promising hydrolysis kinetics with half-life times of 10 h at pH5.0 and 15 days at pH7.4 [11]. To overcome the reduced biodegradation of modified cellulose, we propose the acetalization of cellulose as the first fully reversible chemical modification of cellulose, leading to improved processability along with accelerated biodegradation as the acetal linkers hydrolyze under mild conditions. Our general protocol uses vinyl ethers without the need for metal catalysts or transacetalization agents (Scheme 1), which are typically used to generate acetals from vinyl ethers and alcohols [12,13]. The variety of available vinyl ethers [14] allows adjustment of material properties such as T_g, Young's modulus, elongation at break, or hydrophilicity of the cellulose-based plastics. Polymer solubility in common organic solvents (alcohols, toluene, dichloromethane (DCM), etc.) enables convenient processing of the resulting cellulose acetals, e.g. via drop casting. Finally, we proved that cellulose acetals are stable at room temperature, but degrade at elevated, i.e. typical composting temperatures, as the acetals are cleaved by mild acidic hydrolysis which is an ubiquitous condition during composting [15]. After hydrolysis, native cellulose is released, which is fully degraded by cellulases. We believe that the reversible acetalization of cellulose leads to a new class of bio-based and fully biodegradable polymers for a more sustainable future and prevents further microplastics pollution.

2. Experimental section

2.1. Materials

Benzene-d_6 (≥99 atom%, Deutero GmbH); 1-butyl-3-methylimidazolium chloride (BMIMCl, ≥98 %, Acros) was stored in a desiccator over phosphorous pentoxide (≥98 %, Sigma-Aldrich) before usage; butyl vinyl ether (≥98 %, stabilized with potassium hydroxide, TCI chemicals); cellulase from Trichoderma viride (3–10 units/mg Sigma-Aldrich); cellulose microcrystalline (SigmaCell Cellulose Type 20, 20 μm, Lot#: SLBVV6516, Sigma-Aldrich); 2-chloro-4,4,5,5-tetramethyl-1,3,2-dioxaphospholane (≥95 %, Sigma-Aldrich); cyclohexyl vinyl ether (≥98 %, stabilized with KOH, TCI chemicals); compost samples (2 weeks old) were provided by a local composting facility (Kompostanlage Frankenthal – Wagner GmbH, 67227 Frankenthal, Germany); chromium (III) acetylacetonate (≥97 %, Sigma-Aldrich); dichloromethane-d_2 (≥99.5 atom%, Sigma-Aldrich); dichloromethane (DCM, ≥99.5 %, VWR); dimethylacetamide (DMAc, ≥99.5 %, VWR); dimethylformamide (DMF, ≥99.8 %, VWR); dodecyl vinyl ether (≥98 %, Sigma-Aldrich); *endo-N*-hydroxy-5-norbornene-2,3-dicarboximide (≥99 %, Sigma-Aldrich); lithium chloride (dried at 70 °C under vacuum before usage, ≥98 %, TCI chemicals); methanol (≥99.8 %, VWR); pyridine-d_5 (≥99.5 atom%, Deutero GmbH); 1,1,2,2-tetrachloroethane (≥98 %, Sigma-Aldrich); p-toluenesulfonic acid (pTsOH, ≥98.5 %, Sigma-Aldrich); trifluoroacetic acid (≥99 %,Sigma-Aldrich).

2.2. Acetalization of cellulose

2.2.1. Cellulose butyl acetal and cellulose cyclohexyl acetal

Synthesis of the butyl and cyclohexyl acetal was carried out in the solvent mixture of BMIMCl and DMF. Microcrystalline cellulose (3.2 g, 59.2 mmol OH groups) was transferred in to a 250 mL round bottom flask. In the case of cellulose butyl acetal BMIMCl (40 g, stored over phosphorous pentoxide before usage) together with an elliptical stirring bar was added. The flask was transferred into an oil bath at 60 °C and the solid mixture was gently stirred overnight under vacuum (0.02 mbar) in order to remove residual water from the materials. The next day, the flask was purged with dry nitrogen and dry DMF (72 mL) was added. The oil bath temperature was raised to 80 °C. After 4 h, most of the cellulose was typically dissolved in the mixture and butyl vinyl ether (48 mL, 377 mmol) was added. In the case of cyclohexyl vinyl ether, the procedure was the same, but BMIMCl (68 g) was used together with DMF (57 mL) and (21 mL, 148.2 mmol) of cyclohexyl vinyl ether. After 1 h, the reaction mixture typically cleared up. After 2–3 h, the mixture started to become turbid again. The reaction mixture was further stirred at 80 °C for 72 h and a clear red–orange solution was obtained together with a second viscous phase. The mixture was precipitated in methanol (1 L) under vigorous stirring, while a beige-yellow precipitate was obtained, which stuck to the stirring bar and to the glass wall after several minutes. The supernatant was decanted, and the precipitate was washed with deionized water, filtered, and dried afterwards under reduced pressure at room temperature. The dried precipitate (8 g) was dissolved in DCM in order to gain an 8 wt% polymer solution. The polymer solution was filtered via a syringe filter (pore size: 5 μm) in order to remove insoluble solids and precipitated again in 600 mL methanol. Typically, an off-white to colourless solid polymer was obtained after the second precipitation. The precipitation bath was transferred into 250 mL centrifuge vials and centrifuged at 6000 rcf for 10 min. Methanol was decanted and the polymer was washed again with deionized water and dried under vacuum at 40 °C overnight. Typically, 6.1 ± 0.3 g polymer was obtained for cellulose butyl acetal and cellulose cyclohexyl acetal.

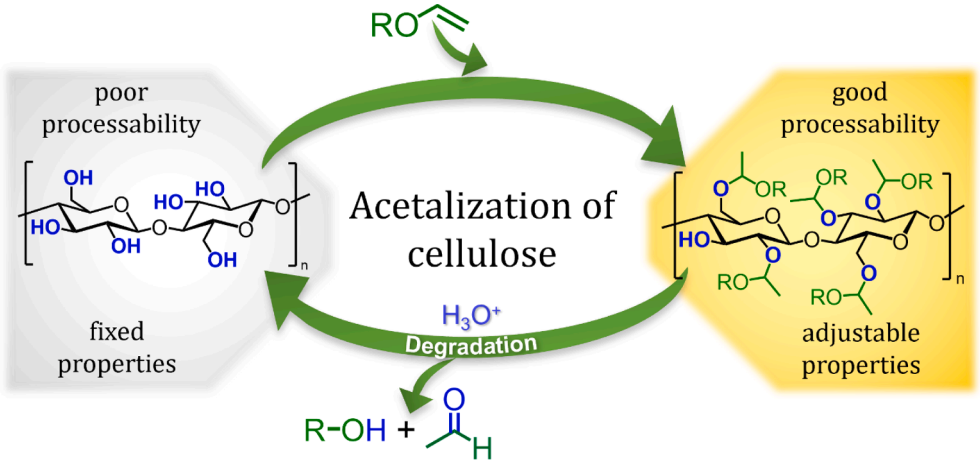

Scheme 1. Concept of the reversible modification of cellulose to the new material class of cellulose acetals. Acetalated cellulose shows solubility in common organic solvents and uncomplicated processability. The acid catalyzed hydrolytic cleavage back to unmodified cellulose ensures full biodegradation of cellulose acetals.

2.2.2. Cellulose dodecyl acetal

Synthesis of the dodecyl acetal was carried out in the solvent mixture of DMAc and LiCl. LiCl (21 g) and DMAc (373 g) was added to a 1 L round bottom flask. After LiCl was fully dissolved at 80 °C, the flask was cooled to room temperature and cellulose (5.3 g) was added while stirring vigorously. Afterwards, the flask was purged with nitrogen and the oil bath temperature was raised to 120 °C for 3 h. Then, the mixture was stirred at room temperature overnight and a yellow-orange cellulose solution was obtained. The solution was stored at room temperature afterwards for several days while a small fraction of insoluble cellulose sedimented at the bottom of the flask and the solution cleared up. This cellulose solution (75 g, approx. 16.5 mmol cellulosic OH groups) was decanted in a 250 mL round bottom flask and fresh DMAc (37.5 g) was added to the solution. The flask was stirred at 750 rpm with an elliptical stirring bar and the oil bath temperature was raised to 85 °C. Afterwards, pTsOH (48 mg, 0.27 mmol) and dodecyl vinyl ether (12.98 mL, 50 mmol) were added to the mixture and the solution was stirred for 72 h at 80 °C. Subsequently, a red–orange solution was obtained together with a yellow viscous phase, which stuck to the glass wall. The red–orange solution was discarded and the yellow viscous polymer phase was precipitated in methanol (300 mL) under vigorous stirring. The yellow precipitate stuck quickly to the stirring bar and to the glass wall. The cleared-up supernatant was decanted and the precipitate was washed with fresh methanol and deionized water five times under vigorous mechanical stirring while the polymer became more and more colourless. The viscous polymer was dried under vacuum at 40 °C overnight and 3.25 g of cellulose dodecyl acetal could be obtained.

2.3. Nuclear magnetic resonance (NMR) spectroscopy

^{1}H and ^{31}P nuclear magnetic resonance (NMR) spectroscopy was performed at a Bruker Avance III system at 400 MHz. For ^{1}H-NMR, 20–30 mg of cellulose acetal polymer was dissolved in 700 μL deuterated dichloromethane and transferred into a NMR tube.

^{13}C CP-MAS solid-state NMR was performed on a Bruker Avance III console operating at 500.2 MHz ^{1}H Larmor frequency using a commercial double-resonance MAS NMR probe supporting zirconia rotors with 2.5 mm outer diameter.

2.4. Determination of degree of substitution via ^{31}P-NMR spectroscopy

The remaining OH group content in the synthesized cellulose acetals was determined by a derivatization technique with 1,3,2-dioxaphospholanyl derivatives and ^{31}P-NMR, according to a slightly modified literature protocol: [16,17] For cellulose cyclohexyl acetal and cellulose butyl acetal, pyridine-d_5 (150 μL) was added to the cellulose acetal (20–35 mg). Afterwards, 1,1,2,2-tetrachloroethane (500 μL) was added to the mixture until everything was dissolved at room temperature. Then, a solution (125 μL, 0.12 M) of endo-N-hydroxy-5-norbornene-2,3-dicarboximide in 1,1,2,2-tetrachloroethane/pyridine-d_5 1:1.6 (v/v) was added as an internal standard. Afterwards, 2-chloro-4,4,5,5-tetramethyl-1,3,2-dioxaphospholane (100 μL, 0.63 mmol) was added to the solution. Finally, a solution of chromium(III) acetylacetonate (50 μL, 50 mM) was added as relaxation agent. The solution was stirred for three minutes until everything was homogeneously dissolved, then 700 μL of the mixture was transferred into an NMR tube. In the case of the more hydrophobic cellulose dodecyl acetal, tetrachloroethane was replaced by deuterated benzene, in order to achieve full dissolution of the polymer. Precipitated pyridinium hydrochloride was separated from the polymer solution by centrifugation at 10 000 rcf for 5 min, then 700 μL of the supernatant was analyzed.

2.5. Infrared spectroscopy

Fourier-transformed infrared spectroscopy (FT-IR) was performed with a Bruker Alpha-P ATR spectrometer.

2.6. Gel permeation chromatography

GPC experiments were performed using an PSS SECcurity^{2} instrument consisting of a pump, autosampler, and column oven. Eluent toluene was used in the analysis of cellulose acetals. A column set consisting of three columns —SDV 106 Å, SDV 104 Å and SDV 500 Å (PSS Standards Service GmbH, Mainz, Germany), all of 300 × 8 mm and 10 μm average particle size were used at a flow rate of 1.0 mL/min and a column temperature of 30 °C. The injection volume was 100 μL. The samples having 1 mg/ml concentration were filtererd prior to measurement through 0.45 μm PTFE filter. Detection was accomplished with a refractive index (RI) detector. Eluent DMAc/0.9 wt% LiCl were used in the analysis for unmodified cellulose and cellulose cyclohexyl acetal. A column set consisting of three columns — GRAM 30 Å, 1000 Å and 1000 Å (PSS Standards Service GmbH, Mainz, Germany) — all of 300 × 8 mm and 10 μm average particle size were used at a flow rate of 1.0 mL/min and a column temperature of 80 °C. The samples having 1 mg/ml concentration were filtererd prior to measurement through 0.45 μm PTFE filter. The injection volume was 200 μL. Detection was accomplished with a RI detector. Data acquisition and evaluation were performed using the PSS WinGPC UniChrom (PSS-Polymer Standards Service GmbH, Mainz, Germany). Calibration was carried out using polystyrene standards provided by the PSS-Polymer Standards Service GmbH (Mainz, Germany).

2.7. Thermogravimetric analysis (TGA)

Thermogravimetric analysis was performed on a Mettler Toledo TGA/DSC 3+ in a nitrogen atmosphere. 5–15 mg of the sample were analyzed in a temperature range of 25–600 °C with a heating rate of 10 K min^{-1}.

2.8. Differential scanning calorimetry (DSC)

The thermal properties of cellulose materials were measured by differential scanning calorimetry (DSC) on a Mettler Toledo DSC 823e calorimeter. Three scanning cycles of heating–cooling–heating in the temperature range −100 °C to +185 °C were performed in an N_2 atmosphere (30 mL/min), with heating and cooling rates of 15 °K/min and 30 °K/min, respectively. 20–40 mg of sample was used for each measurement.

2.9. Mechanical testing

For mechanical testing, cellulose butyl acetal and cellulose cyclohexyl acetal films were prepared on a flat Teflon substrate. Therefore, 5 wt% solutions of cellulose acetals in DCM were prepared. The polymer solutions were degassed in the ultrasonic bath for 5 min and were stored without agitation for 24 h before usage. Afterwards, the polymer solutions were homogeneously casted on the Teflon substrate. The solvent was evaporated under a dry stream of nitrogen for at least 2 h and then for 2 h under vacuum at 50 °C. Dog-bone-shaped samples (with 50 mm gauge length and 4 mm width) were cut from the dried films.

Stress–strain behaviour was studied using a Zwick Z005 universal testing machine. Samples were strained with a pre-load of 0.05 N at room temperature and an extension rate of 2.5 mm min^{-1}.

Rheology experiments were performed using an Advanced Rheometric Expansion System (ARES, Rheometric Scientific). Oscillatory shear deformation was applied under conditions of controlled deformation amplitude, which was kept in the range of the linear viscoelastic response of the studied samples.

2.10. Static water contact angle measurement

Static water contact angle measurements were performed on a DataPhysics contact angle system OCA 15 plus (Germany), equipped

with an electronic syringe unit. Therefore, cellulose acetals were dissolved in DCM to a concentration of 5 wt%. The solutions were filtered via a 0.2 μm syringe filter, degassed for 5 min in an ultrasonic bath and stored for several days without agitation. Afterwards, 400 μL of polymer solution were drop casted on a round 25 mm cover slip. After drop casting, the samples were immediately transferred under a dry nitrogen stream in order to evaporate the solvent in dry conditions for at least 2 h, followed by 2 h under vacuum at room temperature. A 2 μL sessile droplet was deposited on the dried film surface. The drop contour was fitted by the Young-Laplace equation for at least 5 different measurement spots on each film.

2.11. Atomic force microscopy (AFM) imaging

The AFM (MultiMode 8 with NanoScope V controller; Bruker) was operated in the PeakForce Quantitative Nanomechanical Mapping mode (PF-QNM) to record force-distance curves, which were further processed in the NanoScope Analysis software (version 3.0) for data evaluation. The ScanAsyst settings in the operating software (NanoScope, version 9.70) were set to "off" in order to apply dedicated scanning parameters, particularly the feedback loop gain and the applied load, for imaging films of different stiffness. The force-distance curves were collected following a sine-wave sample-tip trajectory with a frequency of 2 kHz and utilizing a peak-force amplitude value 50–150 nm. Medium-soft AFM cantilevers were used with a nominal spring constant of 2 N/m and a tip with a nominal radius of 9 nm (Olympus, OMCL-AC240TS). AFM data were captured in air and at room temperature.

2.12. Degradation test

For degradation studies cellulose acetal films were prepared on 25x25 mm microscopic coverslips. Therefore, 10 wt% solutions of cellulose acetals in DCM were prepared. The polymer solutions were degassed in the ultrasonic bath for 5 min and were stored without agitation for 24 h before usage. Afterwards, 200 μL of the polymer solutions were drop casted with a micropipette on the coverslips. The solvent was evaporated under a dry stream of nitrogen for at least 2 h and then for 2 h under vacuum at 50 °C. The weight of the obtained films was 23 ± 2 mg.

2.13. Scanning electron microscopy

Cellulose acetal films were glued on carbon tape and gold-sputtered to avoid degradation and charging effects (JEOL JFC-1300 Auto Fine coater). Sputtered films were imaged with an JEOL JSM-7610FPlus secondary electron microscope. An acceleration voltage of 1.5 kV and a working distance of 8.0 mm was applied.

2.14. Degradation in aqueous environment

The polymer films with the cover slips were placed in glass vials (V = 100 mL, DIN45, outer dimensions: h = 85.5 mm, d = 45 mm, Dijkstra Vereenigde, the Netherlands) and 4 mL of 0.1 M buffer solutions were added (acetate buffer at pH4, acetate buffer at pH5, phosphate buffer at pH8 and acetate buffer at pH5 with 0.63 U/mL cellulase). The vials were tightly closed, and the samples were incubated at room temperature and in an oven at 58 °C. The samples were not agitated during the experiment. Every third day, the buffer solutions were removed with plastic pipettes. The polymer films were washed thrice with 4 mL deionized water, dried under vacuum at 50 °C for 3 h, and weighed.

2.15. Degradation in compost

Degradation experiments in compost environment followed an adapted protocol from ISO 20200:2015 [18,19]. All compost experiments were conducted in triplicates. Therefore, 2 weeks old compost samples from a local industrial composting facility (Wagner GmbH, 67227 Frankenthal, Germany) were utilized. Large pieces (d > 2 cm) were manually removed. The compost samples exhibited a pH value of 6.8 which was determined by immersing 2 g of compost in with 10 mL deionized water for 30 min and measuring the pH value of the water phase afterwards with a pH electrode.

Wide neck bottles (V = 100 mL, DIN45, outer dimensions: h = 85.5 mm, d = 45 mm, Dijkstra Vereenigde, the Netherlands) with a polypropylene screw cap were chosen as composting containers during the experiment. To ensure oxygen supply to the compost, 6 holes (d = 0.9 mm) were drilled in each screw cap. The polymer films without the cover slips were placed in the bottle together with 8.5 g of compost. The bottles were closed and incubated in an oven at 58 °C. The water content in the compost samples was adjusted to 55 wt%. Every third day, the evaporated water was replaced by deionized water. For every data point, the foils were gently separated from the compost and washed at least 3 times in 10 mL deionized water to remove compost residues. In case of still adherent compost, the foils were immerged in deionized water and placed in a sonication bath for 5 min. Afterwards, the foils were first dried on a paper tissue and afterwards under vacuum at 50 °C for 3 h. The weight after drying was monitored over three months.

3. Results and discussion

3.1. Acetalization of cellulose

The hydroxyl groups of cellulose were modified with vinyl ethers into the respective acetals. The acetalization was performed in solution either using an ionic liquid or LiCl/DMAc as the solvent. Depending on the solubility of the corresponding vinyl ether, the solvent system for the acetalization reaction was adjusted (Fig. 1a). When cyclohexyl vinyl ether or butyl vinyl ether was used as a reagent, the ionic liquid 1-butyl-3-methyl-imidazolium-chloride (BMIMCl) was applied and DMF was added as a co-solvent to reduce the viscosity of the reaction mixture and ensure miscibility with these (more polar) vinyl ethers. For the reaction with the non-polar dodecyl vinyl ether, a solvent mixture consisting of DMAc/LiCl together with pTsOH as the catalyst were used as previously reported [12,16]. Under these conditions, the reagents were solubilized during the reaction and no metal catalysts were needed to perform the acetalization [13]. After the maximum degree of substitution was reached, the cellulose acetals precipitated from the liquid reaction mixture and were easily recovered and separated from the solvent by decanting the solvents in nearly quantitative yields. All cellulose acetals were water-insoluble hydrophobic materials, but were soluble in common organic solvents like dichloromethane, chloroform, toluene, acetone, or isopropanol.

3.2. Characterization

The successful functionalization of the cellulose backbone with the corresponding vinyl ether was proven by a combination of techniques; FT-IR spectroscopy indicated the presence of CH_2 and CH_3 groups in all cellulose acetals with the antisymmetric stretch vibration at ca. 2921–2933 cm^{-1} and a symmetric stretch band at 2852 – 2872 cm^{-1}. Moreover, the acetalization of the hydroxyl groups corresponded to a decrease of the OH stretch vibration at 3600–3040 cm^{-1} from a broad band in the spectrum of unmodified cellulose to a small band at 3474 cm^{-1} in the spectra of the cellulose acetals. Furthermore, an additional band at 1134 cm^{-1}, indicated the introduction of the additional acetal groups in the reaction products.

Solid state ^{13}C-NMR spectroscopy further verified the successful acetalization of cellulose. Resonances between 106 ppm and 64 ppm can be assigned to the anhydroglucose unit of the cellulose backbone [20]. While unmodified cellulose did not exhibit any resonances for aliphatic groups between 0 and 40 ppm, the cellulose acetals proved intense resonances for the aliphatic chains (at 14–34 ppm assigned to CH_2 and

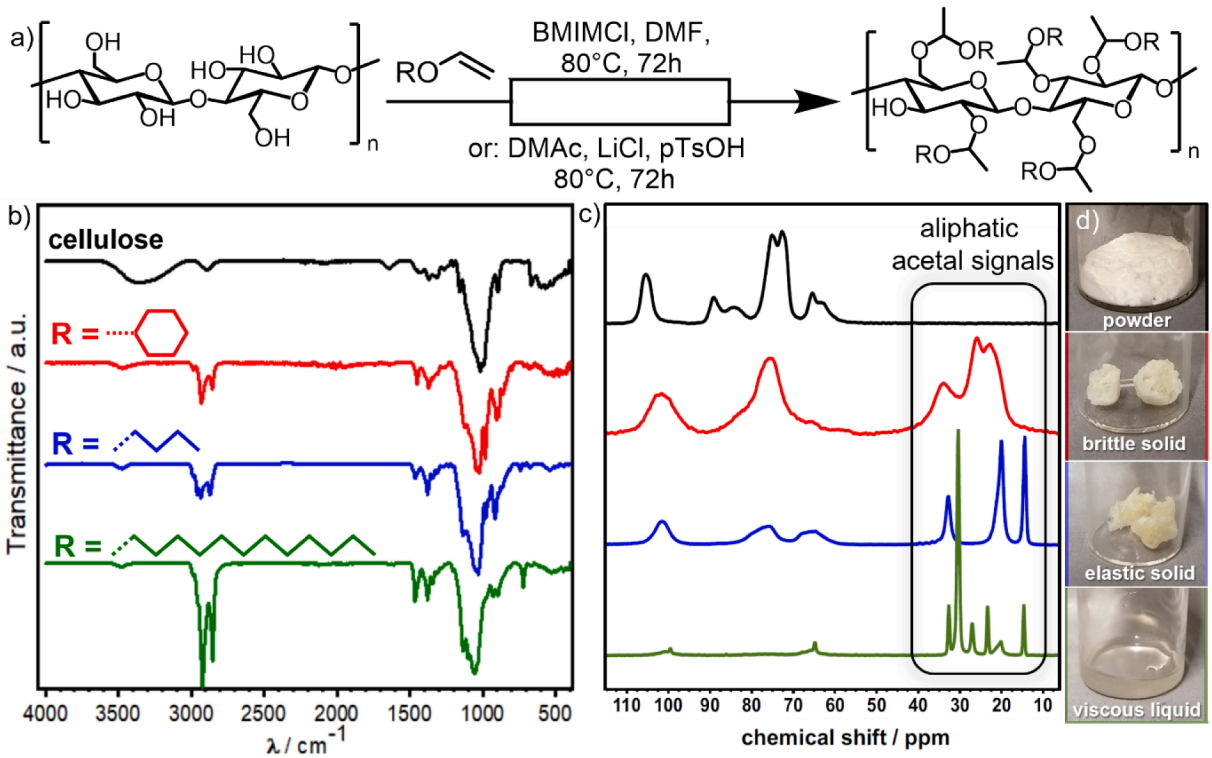

Fig. 1. Synthesis of cellulose acetals. a) Reaction scheme for the acetalization of cellulose; either the solvent system BMIMCl/DMF (for R = cyclohexyl, butyl), or DMAc/LiCl (for R = dodecyl) were used. b) FT-IR spectra of the cellulose acetals in comparison to unmodified cellulose. FT-IR spectra were normalized to the C—O stretch band of the anhydroglucose unit (AGU) at 1015–1050 cm^{-1}. c) Solid state ^{13}C CP-MAS-NMR spectra of the different cellulose acetals compared to unmodified cellulose. d) Comparison of the optical images of the unmodified cellulose powder and the cellulose acetals after precipitation and purification.

CH_3 carbons of the linked acetal chain.

The degree of substitution (DS) of cellulose was determined via a phospholane-based derivatization protocol of the hydroxyl groups followed by the detection of the ^{31}P-NMR-signal in relation to an internal standard (Fig. S1). Following a modified protocol from literature [17], degrees of substitutions in the range from 2.1 ± 0.2 for the cellulose cyclohexyl acetal, 2.6 ± 0.2 for the butyl derivative and 2.7 ± 0.3 for the cellulose dodecyl acetal were determined (Table 1). The difference in DS we attribute to different solubility profiles of the cellulose acetals during the derivatization but was not further optimized.

Size exclusion chromatography revealed that the peak molecular weight of the cellulose acetals was similar compared to unmodified cellulose, indicating no degradation or decomposition of the polymer backbone during the acetalization (Fig. S2).

3.3. Material properties

An interesting tunable material property of cellulose acetals was the water contact angle, which turned out to be highly dependent on the acetal substituent (Fig. 2d). All cellulose acetal films were drop-cast from a DCM solution and dried under a dry nitrogen flow. Homogenous flat surface morphology with root mean square roughness, R_{rms}, values of 8, 3, and 5 nm for cellulose butyl acetal, cellulose cyclohexyl acetal, and cellulose dodecyl acetal were confirmed via AFM (Fig. S3a-c), respectively. While unmodified cellulose films exhibit a static water contact angle of 50 ± 2° with a tendency for droplet spreading and water absorption, cellulose acetals showed a significantly higher contact angle due to the hydrophobicity of the attached aliphatic acetal groups and no droplet spreading was observable during the contact angle measurements. Within the cellulose acetals, hydrophobicity could be tuned over a wide range from 68 ± 3° for the cyclohexyl acetal, to 98 ± 2° for butyl acetal up to 124 ± 3 °C for the dodecyl acetal. Interestingly, cellulose butyl acetal and cellulose cyclohexyl acetal were capable of forming honeycomb structured porous polymer films when drop-casted in humid air. The so-called “breath-figures” (Fig. S3d,e,g,h) were proven by AFM imaging. Therefore, further research and future applications of cellulose acetals in functional surfaces could be expected [21–23].

Table 1
Degree of substitution for the different cellulose acetals and unmodified cellulose (determined according the method by King et al. [17]).

Sample	cellulose	cyclohexyl acetal	butyl acetal	dodecyl acetal
Degree of substitution	0.0	2.1 ± 0.2	2.6 ± 0.2	2.7 ± 0.3

Differences in thermal and mechanical properties of the synthesized cellulose acetals were observable already with the naked eye: unmodified cellulose usually appears as a powder. Due to many hydrogen bonds in the network, no glass transition temperature can be observed by differential scanning calorimetry as reported previously for cellulose (Fig. 2b) [24]. In contrast, cellulose dodecyl acetal was obtained as a very viscous liquid at room temperature, with an accompanying T_g of −48 °C. The low T_g indicates that the dodecyl chain introduces high side-chain flexibility into the polymer network which efficiently prohibits the formation of hydrogen bonds between the single AGU units. In comparison, cellulose butyl acetal is an elastic solid at room temperature with a significantly increased T_g = +45 °C, attributed to the introduction of a shorter butyl chain into the network. With the introduction of the more rigid cyclohexyl substituent, the T_g of the cellulose cyclohexyl acetal can be further increased to +80 °C, which is comparable to glass transition temperatures of common polymers such as PVC, PET or PLA [25,26].

The thermal stability of the cellulose acetals, determined by thermogravimetry, showed that all samples remained stable up to a minimum onset temperature $T_{5\%}$ = 245 °C (Fig. 2a). While unmodified

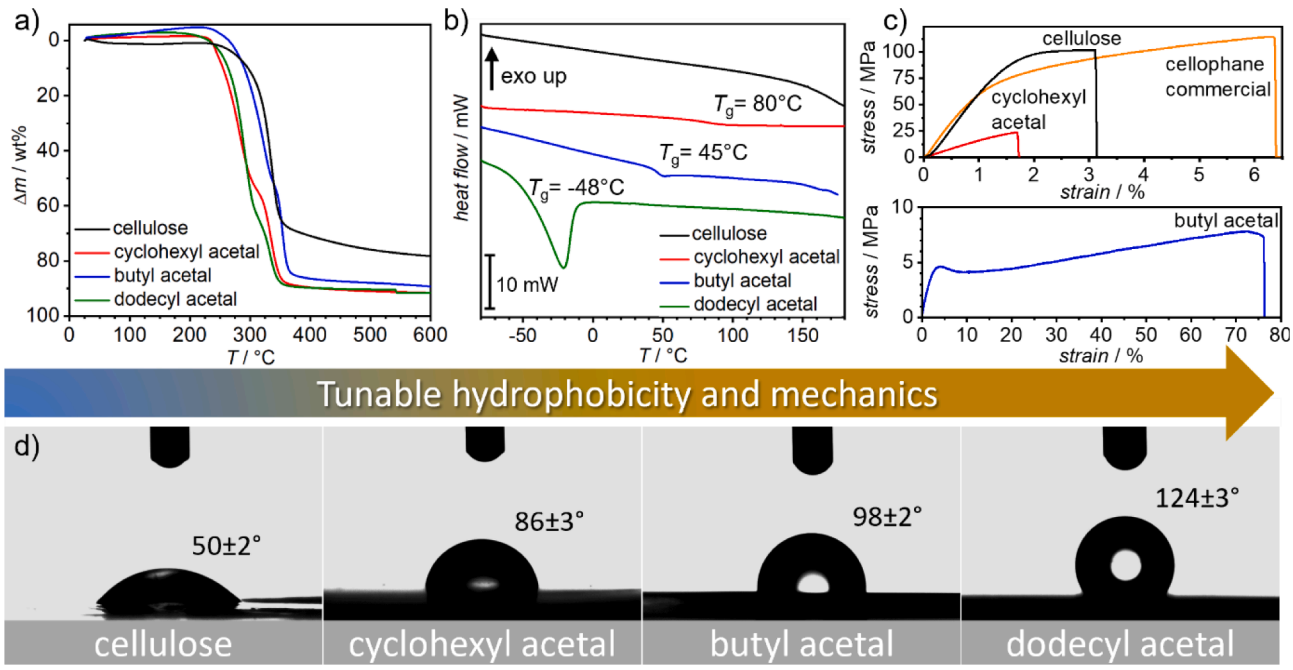

Fig. 2. Material properties of cellulose acetals. a) Thermogravimetric analysis (heat rate: 10 °C/min, under N_2) for cellulose acetals. b) Differential scanning calorimetry (2nd heating curve, heat rate 15 °C/min under N_2). c) Tensile strength measurement of the different cellulose and cellulose acetal films. d) Water contact angle measurement of the different films in comparison. Contact angle data were acquired at least at 5 different measurement spots on each film and standard deviations were calculated.

cellulose started to decompose at $T_{5\%}$ = 275 °C, the acetal modified celluloses, exhibited a 30 °C lower stability, probably because of less hydrogen bonding. The cellulose dodecyl acetal and cellulose cyclohexyl acetal started to degrade at $T_{5\%}$ = 252 °C and 245 °C, respectively. Cellulose butyl acetal exhibited a slightly higher onset degradation temperature of the synthesized acetals at $T_{5\%}$ = 280 °C. Furthermore, the char yield at 600 °C for all cellulose acetals were significantly reduced from 22 % for native cellulose to 11 % for cellulose butyl acetal and 9 % for the cyclohexyl- and dodecyl derivative. The reduced char yield is in accordance with other aliphatic cellulose modifications previously reported [27].

Different mechanical properties of the synthesized cellulose acetals are also characterized by different stress–strain curves (Fig. 2c). Following a literature protocol [28], unmodified cellulose foils were fabricated as reference materials. Commercial cellophane films were used as a second reference material. Each material was measured repeatedly and the average values with their standard deviations were calculated (Table 2). The unmodified cellulose films and commercial cellophane foil were characterized by a Young's modulus of 58 ± 7 MPa and 68 ± 5 MPa, respectively. Cellulose acetals films were characterized by a decrease in the value of Young's modulus (16.0 ± 0.3 MPa for cyclohexyl acetal and 1.9 ± 0.1 MPa for butyl acetal) which can be explained by the reduced hydrogen bonding between hydroxyl groups in the cellulose backbone. Interestingly, the elongation at break of cellulose butyl acetal was significantly increased to 73 ± 8 %, compared to 3.0 ± 0.2 % for the unmodified cellulose films, whereas cellulose cyclohexyl acetal was more brittle and broke at 1.6 ± 0.2 % elongation. The influence of the different acetal substituents was also visible in the maximum stress. The more rigid cyclohexyl substituent results in a higher maximum stress at 22 ± 2 MPa, compared to the butyl acetal which broke at 7.3 ± 0.9 MPa. In contrast, unmodified cellulose broke at a maximum stress of 95 ± 6 MPa. Cellulose dodecyl acetal was characterized with a rheometer due to its low T_g and exhibited a storage modulus of 1.6 $\cdot 10^{-2}$ MPa and a loss modulus of 2.1 $\cdot 10^{-2}$ MPa. Decreased Young's modulus and increased elongation at break are in accordance with the literature reporting derivatized cellulose, e.g. cellulose esters with different DS [27,29,30]. Generally, higher DS leads to decreased Young's modulus, due to less hydrogen bonds in the network. Therefore, adjusting the DS of cellulose acetals is expected to be utilized for further fine tuning of the mechanical properties in future studies.

Table 2
Mechanical characterization data of the synthesized cellulose acetals and unmodified cellulose films. Each film was measured repeatedly and the average values with their standard deviations were calculated.

Sample	Maximum stress/ MPa	Elongation at break/%	Young's Modulus/MPa
cellophane commercial	112 ± 4	6.2 ± 0.3	68 ± 5
unmodified cellulose film	95 ± 6	3.0 ± 0.2	58 ± 7
cyclohexyl acetal	22 ± 2	1.6 ± 0.2	16.0 ± 0.3
butyl acetal	7.3 ± 0.9	73 ± 8	1.9 ± 0.1
	Storage modulus / MPa (0.1 rad/s)	Loss modulus / MPa (0.1 rad/s)	Complex modulus / MPa (0.1 rad/s)
dodecyl acetal	$1.6 \cdot 10^{-2}$	$2.1 \cdot 10^{-2}$	$2.6 \cdot 10^{-2}$

3.4. Polymer degradation

Degradation studies were performed in multiple setups to investigate the proposed two-step degradation. The mechanism consists of a hydrolysis step of the acetal linkages, followed by an enzymatic degradation of the released cellulose. Acetals are known for their lability in acidic conditions leading to the corresponding alcohol and acetaldehyde as degradation products (Fig. 3a) [11,31–33]. Following this idea, the stability of the cellulose cyclohexyl acetal was studied first as proof of concept via ^{1}H-NMR in solution monitoring the release of acetaldehyde (Fig. 3b). Cellulose acetals were stable in non-acidic solvents like dichloromethane over at least several days and the NMR spectra remained unchained. Stability in organic solvents provides the base for

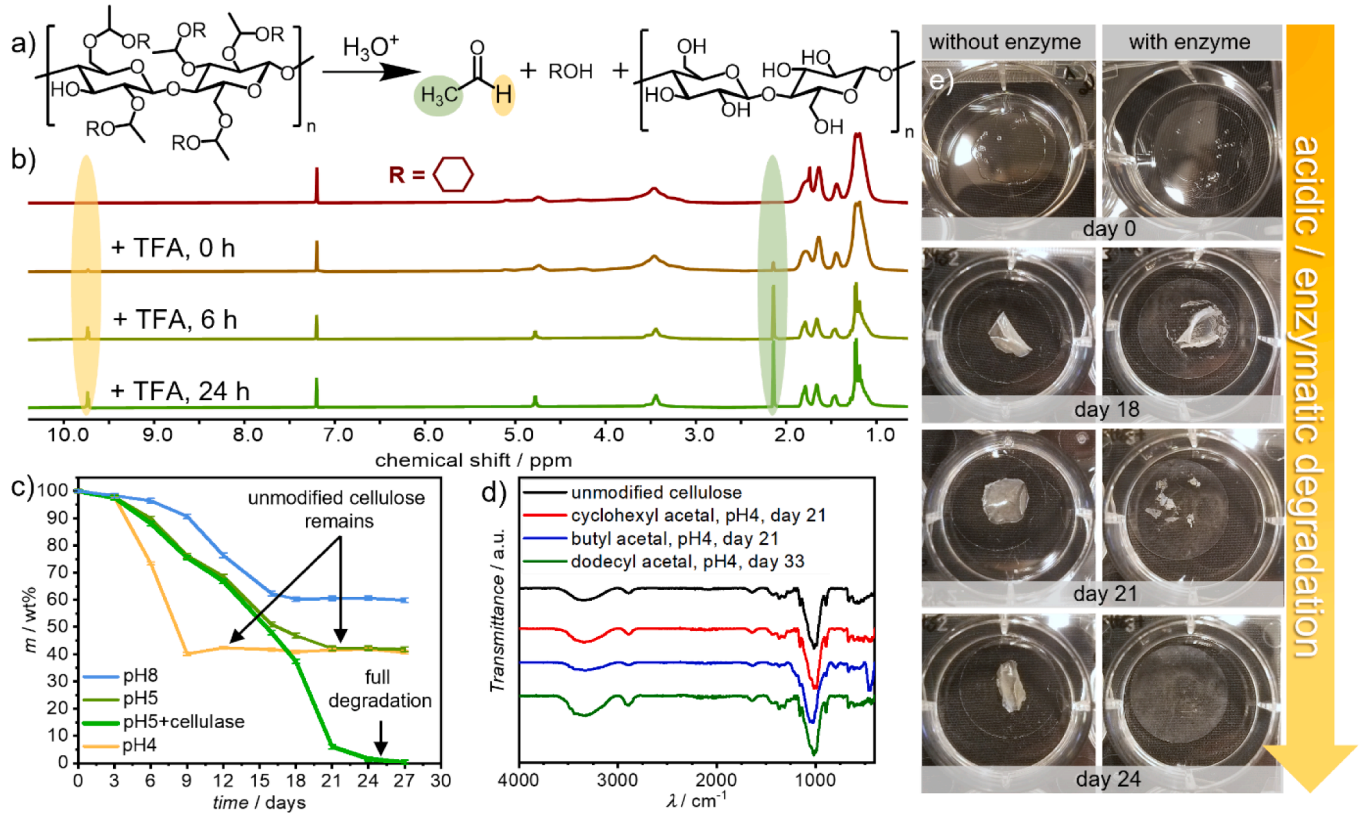

Fig. 3. Degradation of cellulose acetals in aqueous environment. a) Hydrolysis mechanism of the acetal-modified cellulose. b) Hydrolysis kinetics of cellulose cyclohexyl acetal in $CDCl_3$ determined by ^{1}H-NMR spectroscopy using trifluoroacetic acid as a catalyst. c) Gravimetric weight loss of cellulose cyclohexyl acetal film in aqueous media at different pH. Error bars are the standard deviation of the monitored weight loss. d) FT-IR spectra of the different cellulose acetals films after acidic hydrolysis at pH4. e) Optical images of a cyclohexyl acetal film during the hydrolysis at pH5 (without addition of enzyme) and the degradation at pH5 in the presence of cellulase. The glass substrates below the films have a diameter of 25 mm.

solution processing of cellulose acetals. However, immediately after the addition of 0.1 µL trifluoro acetic acid (TFA) to the NMR tube, a colorless precipitate occurred, indicating the regeneration of cellulose. The evolution of additional resonances at 2.2 ppm and 9.7 ppm with an integral ratio of 3:1 in the ^{1}H-NMR spectra revealed the release of acetaldehyde from the polymer. Subsequently, the sample was sealed and stored at room temperature and analyzed again after 6 h and 24 h by ^{1}H-NMR, showing significantly increased resonances for acetaldehyde. Cyclohexanol was detected as the second product after cleaving the acetal linker, which was characterized by a narrowed line width of the hydroxy signals at 3.5 ppm and characteristic aliphatic resonances for cycloalkanes between 1 and 2 ppm. In parallel, the increasing signals for acetaldehyde and cyclohexanol went along with accumulating gel-like precipitate in the NMR-tube, indicating the release of native cellulose.

To further investigate the stability profile of the cellulose acetals, drop casted polymer films of 23 ± 2 mg on round cover slips (d = 25 mm) were immersed in aqueous media at different pH-values for 59 days. Mimicking the natural pH range and temperatures during composting [15], pH values between pH4 and pH8 were chosen and the temperature was kept constant at 58 °C. At room temperature all prepared cellulose-acetal films remained intact (<5 wt% weight loss) for at least 154 days. The degradation was investigated with and without cellulase as the natural cellulose-degrading enzyme. Every 3 days, the polymer films were vacuum-dried, and their weight loss was monitored (Fig. 3c and S4). As the optical images show (Fig. 3e), the cellulose cyclohexyl acetal films typically started to detach from the underlying glass substrate and started folding randomly after 3 days. Notably, cellulose cyclohexyl acetal films did not fragment but exhibited a significant weight loss up to 60 ± 1 wt% at pH4 and pH5 (Fig. 3c), which corresponds to the expected weight loss due to a full cleavage of the cyclohexyl substituents in the polymer (Table S1). The half-life times for the hydrolytic acetal cleavage of the cyclohexyl acetal were 6 ± 1 days at pH4 and 11 ± 2 days at pH5 (Table S2). This behaviour could also be observed for the butyl and dodecyl derivative (Fig. S4). The more acidic the degradation environment, the faster the cellulose acetal films lost weight. Native cellulose films did not decompose under these conditions, which was indicated by a constant weight and no disintegration of the film. After 9 days at pH4 or 21 days at pH5, the weight loss of all the cyclohexyl acetal samples stayed constant and the films were analyzed via FT-IR. No significant differences in the FT-IR spectra of the samples after 21 days at pH4 compared to native cellulose could be detected (Fig. 3d). Therefore, native cellulose was proven to be the final residue. These findings also support that in the previously discussed NMR experiments, native cellulose was regenerated as the gel-like precipitate. Remarkably, cellulose cyclohexyl acetal and cellulose butyl acetal lost 40 ± 2 % of their weight even at pH8, indicating a partial acetal hydrolysis most probably of tertiary acetals groups even in mildly basic conditions as reported previously for other acetals in water at pH8 [34–36].

When the films were incubated additionally with cellulase further biodegradation occurred: incubation of the cellulose cyclohexyl acetal films with cellulase at pH5 led to fragmentation of the films from day 18. Before day 18, the polymer films exhibited the same weight loss profile as samples incubated without the enzyme (Fig. 3c), indicating a two-stage degradation profile under these conditions. Initially, the degradation process was dominated by the acetal hydrolysis. Once the acetal bonds were cleaved, the fragmentation quickly continued from day 18 until up to 100 % weight loss was reached after 27 days. In comparison, cellophane films which were incubated in the same condition (pH5 + cellulase) were fully degraded at the first measurement point after 3

days.

Cellulose butyl acetal and dodecyl acetal followed the same degradation mechanism, however with slower degradation kinetics. Full deacetalization at pH5 was achieved after 48 days accompanied with 51 ± 1 wt% weight loss for butyl acetal and 85 ± 1 wt% weight loss for the dodecyl derivative (Fig. S4). The half-life times for the hydrolytic acetal cleavage of the butyl acetal were 13 ± 2 days at pH4 and 23 ± 2 days at pH5 (Table S2). Cellulose dodecyl acetal films also fragmented macroscopically (Fig. S5), indicating again the deacetalization of the polymer. However, monitoring of the weight loss of the dodecyl derivative was afflicted with a larger error because of spreading and the stickiness of the polymer (Tg = -48 °C) to the surrounding, especially at pH8. The corresponding half-life times for the hydrolytic acetal cleavage of the dodecyl acetal were 25 ± 2 days at pH4 and 30 ± 2 days at pH5 (Table S2).

Cellulose butyl acetal films were fully degraded after 59 days when incubated at pH5 together with cellulase. Slower degradation kinetics for butyl and dodecyl compared to the cyclohexyl derivative were expected due to the chemical structure of the acetal substituents: while the cyclohexyl derivative exhibits a tertiary carbon next to the acetal oxygen, the butyl and dodecyl derivatives carry a primary carbon center in this position. An easier protonation of the acetal oxygen next to a tertiary carbon would lead to an increased hydrolysis of the cyclohexyl acetal compared to the butyl and dodecyl derivative, which was reported in other acetal hydrolysis studies before [37]. Moreover, water diffusion might be hindered in case of the dodecyl acetal due to the water insolubility of its degradation product dodecanol, which creates another rate-limiting step for the hydrolysis in these *in vitro* conditions [38].

The degradation of the cellulose acetals was also investigated in realistic compost environment from a local composting facility. The cellulose acetal films were incubated in a two weeks old compost sample and kept at 58 °C, following a slightly modified ISO standard protocol [18,19]. In general, natural compost exhibits a complex composition and varies in the presence of active bacterial and fungal microorganisms secreting the cellulase enzymes. Therefore, the composting setup is

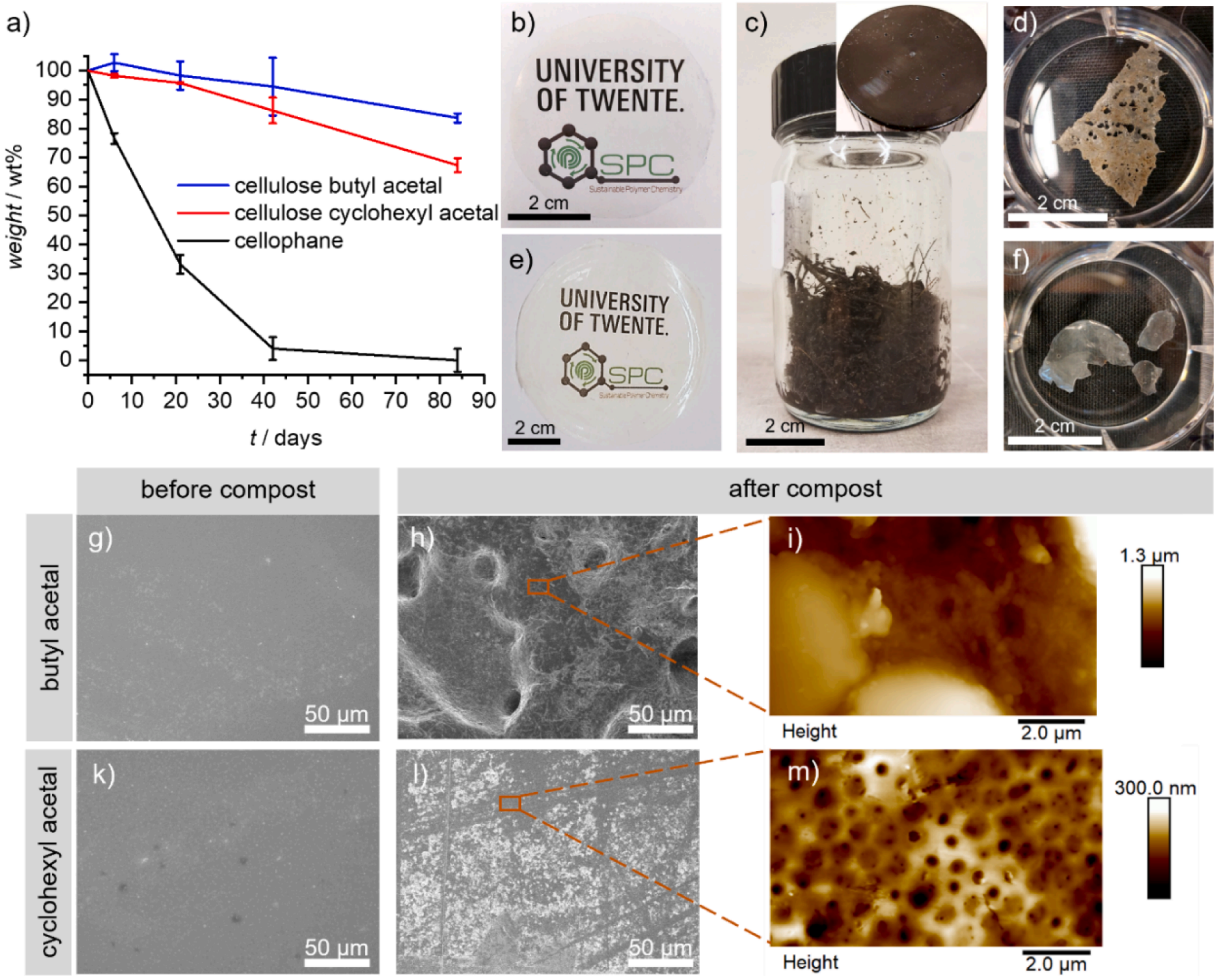

Fig. 4. Degradation of cellulose acetals in compost environment. a) Gravimetric weight loss of cellulose butyl acetal, cellulose cyclohexyl acetal and cellophane films during composting at 58 °C. Samples were incubated in triplicates. Error bars are the standard deviation of the monitored weight loss. b) Translucent cellulose butyl acetal foil before the degradation in compost. c) Laboratory composting container with 6 holes in the lid (d = 0.9 mm) for air supply [18]. Two weeks old compost were obtained from a local composting facility (Wagner GmbH, 67227 Frankenthal, Germany). d) Optical image of cellulose butyl acetal film after 84 days composting. Macroscopic surface erosion and beginning perforation is visible. e) Translucent cellulose cyclohexyl acetal film before composting. f) Cellulose cyclohexyl acetal after 84 days composting. Surface erosion and fragmentation is visible. g) SEM image of the cellulose butyl acetal film before composting. In accordance with Fig. S3a, flat surface morphology is visible (R_{rms} = 8 nm). h) SEM image of the cellulose butyl acetal film after 84 days composting. Rough surface morphology is visible. i) Corresponding AFM image of surface-eroded cellulose butyl acetal film after 84 days of composting. Even on the flattest spots of the sample R_{rms} of 220 nm was determined (increase by factor of 27.5). k) SEM image of the cellulose cyclohexyl acetal film before composting. In accordance with Fig. S3b, flat surface morphology is visible (R_{rms} = 3 nm). l) SEM image of the cellulose cyclohexyl acetal film after 84 days composting. Rough surface morphology is visible. m) Corresponding AFM image of cellulose cyclohexyl acetal film after 84 days composting. Even on the flattest spots R_{rms} of 40 nm was determined (increase by factor of 13.3).

typically afflicted with larger statistical errors compared to the degradation in aqueous conditions. Moreover, the monitored weight losses during the compost setup might be systematically lower because some compost residues stick to the polymer films during the washing procedure. The degradation kinetics of the hydrolytic deacetalization step were expected and observed to be slower because compost is an inhomogeneous solid mixture, which means the surface area, which is in contact with the polymer, is decreased compared to a full immersion in aqueous media. However, surface erosion, perforation and fragmentation of cellulose acetal films were visible, after 6 weeks (Fig. 4d,f), which was accompanied with a weight loss of 5 ± 9 wt% for cellulose butyl acetal and 14 ± 4 wt% for cellulose cyclohexyl acetal. In the following, the degradation of the cellulose acetal films continued with a weight loss of 33 ± 2 wt% for cellulose cyclohexyl acetal and 16 ± 2 wt% for cellulose butyl acetal after 12 weeks (Fig. 4a). The surface of the butyl and cyclohexyl acetal films were further examined with SEM and AFM (Fig. S3a-b and S6 g-m). Drop-casted butyl acetal and cyclohexyl acetal films showed flat surface morphology (Fig. 4g, k and Fig. S3). In contrast, SEM images of the acetal films after 84 days of composting revealed significantly eroded surfaces. Even at the flattest areas of these surfaces, the R_{rms} increased to 220 nm and 40 nm, which corresponds to an increase by factor 27.5 and 13.3, for butyl acetal and cyclohexyl acetal, respectively. Therefore, significant cleavage of acetal groups, accompanied with microscopic and macroscopic surface erosion of the acetal films, were proven in compost as well as in aqueous conditions.

Summarizing our degradation experiments, ^{1}H-NMR analysis together with gravimetric and FT-IR analysis proved that cellulose acetals undergo a two-step degradation mechanism. First, the acetal hydrolysis regenerates native cellulose. The weight loss, caused by acetal hydrolysis was shown in a pH range from pH4 − 8 (as expected in a composting facility) with increasing hydrolysis rates when the pH-value was decreased. Second, the full enzymatic degradation of the regenerated cellulose was shown if cellulases are present. This two-step degradation mechanism was observed in aqueous media as well as in real compost conditions rendering the cellulose acetals a versatile platform technology to fully biodegradable and biobased plastics with controlled stability.

4. Conclusion

This work presents the synthesis of cellulose acetals, a new class of bio-based and fully biodegradable polymers, which are characterized by a high degree of substitution, solubility in common organic solvents, thermal processability, and adjustable material properties. The cellulose acetalization is a straightforward approach to increase cellulose's processability while guaranteeing a full biodegradation by combining a hydrolysis-labile linker to the cellulose backbone. The cellulose functionalization was successfully achieved with different vinyl ethers, rendering our acetalization as a versatile platform and we expect many more cellulose acetals to be synthesized via the proposed synthesis routes. Various commercially available vinyl ethers as well as tailored synthesis protocols for special vinyl ethers [14] enable a broad range of new cellulose-based materials, in which the mechanical properties are expected to be further fine tuneable by an adjusted degree of substitution as reported for other cellulose derivatives before [27]. Moreover, the formation of structured honeycomb polymer films via breath-figures qualifies cellulose acetals for the fabrication of smart functional and biodegradable surfaces [22,23].

Finally, the acetalization is a reversible cellulose functionalization and the synthesized bio-based polymers are biodegradable by a two-step acidic-enzymatic degradation mechanism preventing the formation of recalcitrant microplastic particles. The two-step degradation was proven in aqueous media in a realistic pH-range as well as in real composting environment. We clearly see cellulose acetals at the forefront of modern polymer materials because they provide bio-based and biodegradable alternatives to petroleum-based and non-degradable plastics. Furthermore, we expect many future applications in fields where degradability is an essential part of the function, for instance in drug delivery or agriculture.

Declaration of Competing Interest

The authors declare that they have no known competing financial interests or personal relationships that could have appeared to influence the work reported in this paper.

Data availability

Data will be made available on request.

Acknowledgements

The authors thank Andreas Hanewald (MPI-P Mainz) and Kaloian Koynov (MPI-P Mainz) for technical assistance and advice with the rheology and stress-strain measurements, Sandra Seywald (MPI-P Mainz) and Christine Rosenauer (MPI-P Mainz) for GPC measurements, Robert Graf (MPI-P Mainz) for solid-state NMR, Petra Räder (MPI-P Mainz) for TGA and DSC support and Elke Muth (MPI-P Mainz) for FT-IR measurements. Clemens Padberg (UT) is acknowledged for SEM imaging. Katharina Landfester (MPI-P Mainz) is acknowledged for continuous support.

This work was supported by NWO XS [21.2.054].

Appendix A. Supplementary data

Supplementary data to this article can be found online at https://doi.org/10.1016/j.cej.2022.139280.

References

[1] W.G. Glasser, B.K. Mccartney, G. Samaranayake, Cellulose derivatives with low degree of substitution. 3. The biodegradability of cellulose esters using a simple enzyme assay, Biotechnology Progress 10(2) (1994) 214-219. https://doi.org/10.1021/bp00026a011.

[2] E. Samios, R.K. Dart, J.V. Dawkins, Preparation, characterization and biodegradation studies on cellulose acetates with varying degrees of substitution, Polymer 38 (12) (1997) 3045–3054. https://doi.org/10.1016/S0032-3861(96)00868-3.

[3] N. Yadav, M. Hakkarainen, Degradable or not? Cellulose acetate as a model for complicated interplay between structure, environment and degradation, Chemosphere 265 (2021), 128731. https://doi.org/10.1016/j.chemosphere.2020.128731.

[4] R. Geyer, J.R. Jambeck, K.L. Law, Production, use, and fate of all plastics ever made, Sci. Adv. 3 (7) (2017), https://doi.org/10.1126/sciadv.1700782.

[5] I. Peeken, S. Primpke, B. Beyer, J. Gütermann, C. Katlein, T. Krumpen, M. Bergmann, L. Hehemann, G. Gerdts, Arctic sea ice is an important temporal sink and means of transport for microplastic, Nat. Commun. 9 (1) (2018) 1505, https://doi.org/10.1038/s41467-018-03825-5.

[6] ECHA, Registry of restriction intentions until outcome European Chemical Agency, https://echa.europa.eu/de/registry-of-restriction-intentions/-/dislist/details/0b0236e18244cd73, 2019.

[7] C.-C. Chen, L. Dai, L. Ma, R.-T. Guo, Enzymatic degradation of plant biomass and synthetic polymers, Nat. Rev. Chem. 4 (3) (2020) 114–126, https://doi.org/10.1038/s41570-020-0163-6.

[8] V.K. Varshney, S. Naithani, Chemical functionalization of cellulose derived from nonconventional sources, in: S. Kalia, B.S. Kaith, I. Kaur (Eds.), Cellulose Fibers: Bio- and Nano-Polymer Composites: Green Chemistry and Technology, Springer, Berlin Heidelberg, Berlin, Heidelberg, 2011, pp. 43–60, https://doi.org/10.1007/978-3-642-17370-7_2.

[9] A. Behr, T. Seidensticker, Einführung in die Chemie nachwachsender Rohstoffe (2018), https://doi.org/10.1007/978-3-662-55255-1.

[10] Y. Habibi, Key advances in the chemical modification of nanocelluloses, Chem. Soc. Rev. 43 (5) (2014) 1519–1542, https://doi.org/10.1039/C3CS60204D.

[11] E.M. Bachelder, T.T. Beaudette, K.E. Broaders, J. Dashe, J.M.J. Fréchet, Acetal-derivatized dextran: an acid-responsive biodegradable material for therapeutic applications, J. Am. Chem. Soc. 130 (32) (2008) 10494–10495, https://doi.org/10.1021/ja803947s.

[12] K. Suzuki, S. Kurata, I. Ikeda, Homogeneous acetalization of cellulose in lithium chloride and dimethylacetamide, Polym. Int. 29 (1) (1992) 1–6. https://doi.org/10.1002/pi.4990290102.

[13] K.S. Massone, Veit; D'Andola, Giovanni; Mormann, Werner; Wezstein, Markus; Leng, Wei, Method for porducing cellulose acetals, Germany, 2007 (WO2008003643A1).
[14] R. Matake, Y. Adachi, H. Matsubara, Synthesis of vinyl ethers of alcohols using calcium carbide under superbasic catalytic conditions (KOH/DMSO), Green Chem. 18 (9) (2016) 2614–2618, https://doi.org/10.1039/C5GC02977E.
[15] M.A. Hubbe, M. Nazhad, C. Sánchez, Composting as a way to convert cellulosic biomass and organic waste into high-value soil amendments: A review, BioResources 5 (4) (2010) 2808–2854.
[16] T.O. Machado, S.J. Beckers, J. Fischer, C. Sayer, P.H.H. de Araújo, K. Landfester, F. R. Wurm, Cellulose nanocarriers via miniemulsion allow pathogen-specific agrochemical delivery, J. Colloid Interface Sci. 601 (2021) 678–688. https://doi.org/10.1016/j.jcis.2021.05.030.
[17] A.W.T. King, J. Jalomäki, M. Granström, D.S. Argyropoulos, S. Heikkinen, I. Kilpeläinen, A new method for rapid degree of substitution and purity determination of chloroform-soluble cellulose esters, using 31P NMR, Anal. Methods 2 (10) (2010) 1499–1505, https://doi.org/10.1039/C0AY00336K.
[18] I. Standard, Plastics - Determination of the degree of disintegration of plastic materials under simulated composting conditions in a laboratory-scale test, ISO 20200:2015, International Organization for Standardization (2015) 1–8.
[19] L. Reisman, A. Siehr, J. Horn, D.C. Batiste, H.J. Kim, G.X. De Hoe, C.J. Ellison, W. Shen, E.M. White, M.A. Hillmyer, Respirometry and cell viability studies for sustainable polyesters and their hydrolysis products, ACS Sustainable Chem. Eng. 9 (7) (2021) 2736–2744, https://doi.org/10.1021/acssuschemeng.0c08026.
[20] S. Haslinger, S. Hietala, M. Hummel, S.L. Maunu, H. Sixta, Solid-state NMR method for the quantification of cellulose and polyester in textile blends, Carbohydr. Polym. 207 (2019) 11–16. https://doi.org/10.1016/j.carbpol.2018.11.052.
[21] G. Widawski, M. Rawiso, B. François, Self-organized honeycomb morphology of star-polymer polystyrene films, Nature 369 (6479) (1994) 387–389, https://doi.org/10.1038/369387a0.
[22] S. Falak, B. Shin, D. Huh, Modified breath figure methods for the pore-selective functionalization of honeycomb-patterned porous polymer films, Nanomaterials 12 (7) (2022) 1055.
[23] A. Zhang, H. Bai, L. Li, Breath figure: A nature-inspired preparation method for ordered porous films, Chem. Rev. 115 (18) (2015) 9801–9868, https://doi.org/10.1021/acs.chemrev.5b00069.
[24] E. Esen, M.A.R. Meier, Sustainable functionalization of 2,3-dialdehyde cellulose via the passerini three-component reaction, ACS Sustainable Chem. Eng. 8 (41) (2020) 15755–15760, https://doi.org/10.1021/acssuschemeng.0c06153.
[25] S. Iannace, L. Sorrentino, E. Di Maio, 6 - Biodegradable biomedical foam scaffolds, in: P.A. Netti (Ed.), Biomedical Foams for Tissue Engineering Applications, Woodhead Publishing, 2014, pp. 163–187, https://doi.org/10.1533/9780857097033.1.163.
[26] R.M. Grigorescu, M.E. Grigore, L. Iancu, P. Ghioca, R.-M. Ion, Waste electrical and electronic equipment: a review on the identification methods for polymeric materials, Recycling 4 (3) (2019) 32.
[27] E. Esen, P. Hädinger, M.A.R. Meier, Sustainable fatty acid modification of cellulose in a CO2-based switchable solvent and subsequent Thiol-Ene modification, Biomacromolecules 22 (2) (2021) 586–593, https://doi.org/10.1021/acs.biomac.0c01444.
[28] H. Sadeghifar, R.A. Venditti, J.J. Pawlak, J.S. Jur, Cellulose transparent and flexible films prepared from DMAc/LiCl solutions, Bioresources 14 (2019) 9021–9032.
[29] K.N. Onwukamike, S. Grelier, E. Grau, H. Cramail, M.A.R. Meier, Sustainable transesterification of cellulose with high oleic sunflower oil in a DBU-CO2 switchable solvent, ACS Sustainable Chem. Eng. 6 (7) (2018) 8826–8835, https://doi.org/10.1021/acssuschemeng.8b01186.
[30] C. Satgé, R. Granet, B. Verneuil, P. Branland, P. Krausz, Synthesis and properties of biodegradable plastic films obtained by microwave-assisted cellulose acylation in homogeneous phase, C. R. Chim. 7 (2) (2004) 135–142. https://doi.org/10.1016/j.crci.2003.11.003.
[31] S. Wang, F. Fontana, M.-A. Shahbazi, H.A. Santos, Acetalated dextran based nano- and microparticles: synthesis, fabrication, and therapeutic applications, Chem. Commun. 57 (35) (2021) 4212–4229, https://doi.org/10.1039/D1CC00811K.
[32] K.E. Broaders, J.A. Cohen, T.T. Beaudette, E.M. Bachelder, J.M.J. Fréchet, Acetalated dextran is a chemically and biologically tunable material for particulate immunotherapy, Proc. Natl. Acad. Sci. 106 (14) (2009) 5497–5502, https://doi.org/10.1073/pnas.0901592106.
[33] J. Zhang, Y. Jia, X. Li, Y. Hu, X. Li, Facile Engineering of biocompatible materials with pH-modulated degradability, Adv. Mater. 23 (27) (2011) 3035–3040. https://doi.org/10.1002/adma.201100679.
[34] M.D. Pluth, R.G. Bergman, K.N. Raymond, Catalytic deprotection of acetals in basic solution with a self-assembled supramolecular "nanozyme", Angew. Chem. Int. Ed. 46 (45) (2007) 8587–8589. https://doi.org/10.1002/anie.200703371.
[35] I.E. Markó, A. Ates, A. Gautier, B. Leroy, J.-M. Plancher, Y. Quesnel, J.-C. Vanherck, Cerium(IV)-catalyzed deprotection of acetals and ketals under mildly basic conditions, Angew. Chem. Int. Ed. 38 (21) (1999) 3207–3209. https://doi.org/10.1002/(SICI)1521-3773(19991102)38:21<3207::AID-ANIE3207>3.0.CO;2-I.
[36] N.S. Krishnaveni, K. Surendra, M.A. Reddy, Y.V.D. Nageswar, K.R. Rao, Highly efficient deprotection of aromatic acetals under neutral conditions using β-cyclodextrin in water, The Journal of Organic Chemistry 68 (5) (2003) 2018–2019, https://doi.org/10.1021/jo026482+.
[37] B. Liu, S. Thayumanavan, Substituent effects on the pH sensitivity of acetals and ketals and their correlation with encapsulation stability in polymeric nanogels, J. Am. Chem. Soc. 139 (6) (2017) 2306–2317, https://doi.org/10.1021/jacs.6b11181.
[38] M.J. Heffernan, N. Murthy, Polyketal nanoparticles: A new pH-sensitive biodegradable drug delivery vehicle, Bioconjug. Chem. 16 (6) (2005) 1340–1342, https://doi.org/10.1021/bc050176w.